Phonon anomalies and local atomic displacements in the exchange-enhanced superconductor U_6Fe

C. W. Kimball, P. P. Vaishnava, and A. E. Dwight
Northern Illinois University, DeKalb, Illinois 60115

James D. Jorgensen and F. Y. Fradin
Materials Science and Technology Division, Argonne National Laboratory, Argonne, Illinois 60439
(Received 27 March 1985)

Mössbauer effect and neutron-diffraction measurements have been made as a function of temperature on the exchange-enhanced superconductor U_6Fe. Non-Debye behavior is observed in the thermal mean-squared displacement of Fe with the Debye temperature changing from $\Theta_f \cong 320$ K above 100 K to $\Theta_f \cong 400$ K below 80 K. Changes in the Mössbauer shift below 100 K are attributed principally to electronic-structure changes of the Fe atom which lead to a small increase in the number of d electrons and a concomitant reduction in the number of s electrons. The neutron-diffraction results indicate a pronounced anisotropy in the unit-cell thermal expansion and below 100 K an anomalous temperature dependence for the c-axis component of the total Debye-Waller factor of Fe. These observations taken together imply that along the c axis, static displacements of the Fe atoms begin around 100 K and increase with decreasing temperature.

I. INTRODUCTION

The metallic uranium compounds U_6X (X=Mn, Fe, Co, and Ni) are superconducting with transition temperatures ranging from 3.8 K (U_6Fe) to less than 1 K (U_6Ni).[1] The X composition dependence of T_c is similar to that of the Pauling-Slater curve for saturation magnetization of $3d$ transition-metal alloys, which led Hill and Matthias[2] to conclude that triplet pairing might be playing a role in U_6X superconducting behavior. The superconducting U_6X compounds do not, however, exhibit localized magnetic moment behavior, as does the Kondo system $CeCu_2Si_2$;[3] but the U_6X compounds do show high-field superconductivity and exchange-enhanced paramagnetism[4] similar to materials exhibiting strongly interacting Fermi-liquid behavior.[3,5] Delong *et al.*[4] found U_6Fe to possess a nearly temperature-independent paramagnetic susceptibility comparable in magnitude to Pd. DeLong *et al.*[4] also discovered that this low-T_c system has a remarkably high critical field $H_{c2}(0) \approx 100$ kOe with an initial slope at T_c of 34.2 kOe/K.

A number of systems, e.g., $CeCu_2Si_2$,[3,6] UBe_{13},[7] UPt_3,[8–10] have been recently found to have the striking properties of low T_c and very high H_{c2} values. This behavior has been attributed to the superconducting electrons having "heavy" fermion character. For example, Steglich *et al.*[3] found that for $CeCu_2Si_2$ the normal-state specific-heat extrapolation yields an electronic coefficient of specific heat ($\gamma \approx 1$ J mol^{-1} K^{-2}) that is three orders of magnitude larger than that of a simple metal. This behavior is usually associated with a Fermi-liquid phase in Kondo or mixed-valence systems. The height of the specific heat jump at T_c is found to be commensurate with the large normal-state specific heat; the superconducting state then arises from large effective mass ($m^* \sim 200m$), heavy, Cooper pairs. This in turn implies that the Ce f electrons, which normally would be considered to be the magnetic electrons of the system, are also involved in the superconductivity. From specific heat measurements on U_6Fe, DeLong *et al.*[4] find $\gamma \sim 150$ mJ mol^{-1} K^{-2}; the effective mass of the electrons in the superconducting pairs is estimated to be $m^* \sim 20m$. (On a per U basis γ has a value of ~ 25 mJ K^{-2}, which is comparable to a number of nonsuperconducting uranium compounds.) Hence, U_6Fe appears to be intermediate between the very heavy-fermion systems with strong paramagnetic renormalization and the conventional superconductors with strong electron-phonon renormalization. Isotope effect studies in U_6Fe have been made for iron[11] and uranium.[12] No effect on T_c is found with iron mass; for the uranium mass, $T_c \sim M^{-0.37}$. The resistivity of U_6Fe shows negative curvature at low temperature,[13] similar to that observed in UPt_3 (Ref. 9) and some spin-fluctuation actinide systems.[14]

In the present paper ^{57}Fe Mössbauer-effect and neutron-diffraction measurements were made to study the lattice vibrational properties and structural behavior of U_6Fe.

EXPERIMENTAL

U_6Fe has a body-centered tetragonal structure which is unique to U, Np, and Pu compounds with the magnetic $3d$ elements.[15] U_6Fe forms at a fixed stoichiometry by a peritectic reaction. The compound was prepared by triple-arc-melting high-purity depleted uranium and 99.99%-pure iron; the ingots were annealed for seven days at 650 °C and 700 °C. The material was then powdered and strain annealed. The x-ray patterns were identified as the tetragonal U_6Fe structure. Impurity phases which have been found to occur in this compound are UFe_2, U, and UO_2.[16] No UFe_2 or U, but a small quantity of UO_2,

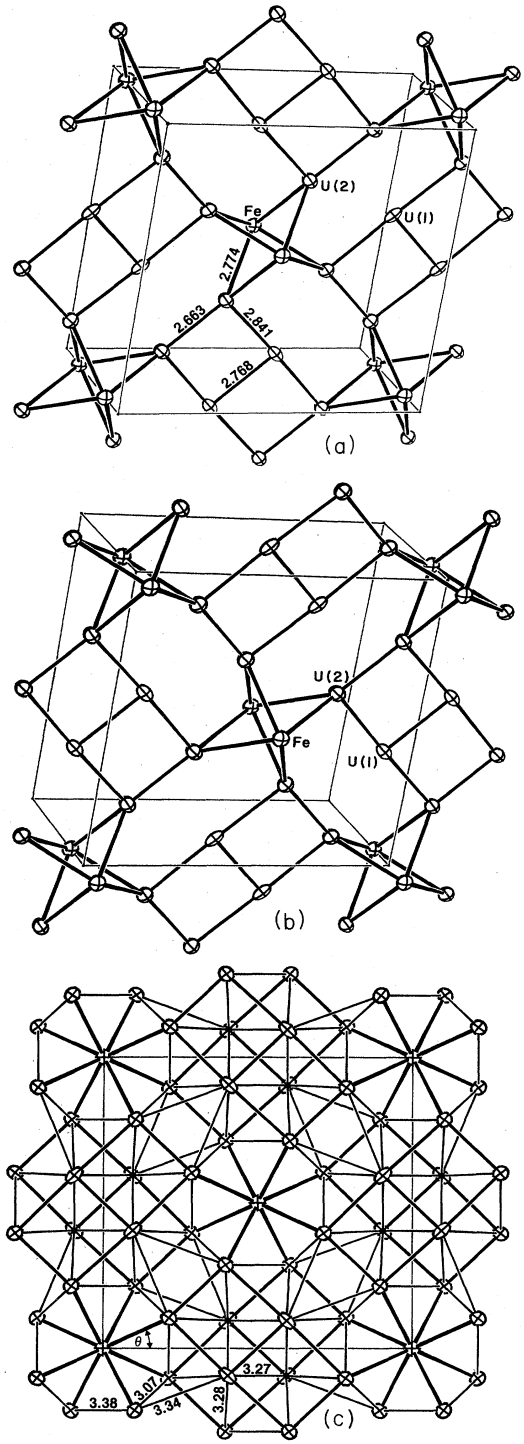

FIG. 1. The body-centered tetragonal structure of U_6Fe. In all views the c axis is into the paper. Bond lengths are in Å. In (a) all of the uranium atoms are in a plane at $z=\frac{1}{2}$. In (b) the uranium atoms are in a plane at $z=0$. The short U—U bonds lie in these planes. Iron atoms are at $z=\frac{1}{4}$ and $z=\frac{3}{4}$ for $x=0$, $y=0$, and $x=\frac{1}{2}$, $y=\frac{1}{2}$. The view in (c) is obtained by combining the layers at (a) and (b) and looking along the $+z$ direction. Except for the 3.34-Å bond the U—U bonds labeled in (c) connect uranium atoms in different layers.

was detected in the x-ray diffraction patterns.

The bct structure has 28 atoms per unit cell. The Fe atoms occur in widely separated chains along the c axis, at the center and corners of the unit cell (Fig. 1). The interatomic Fe-Fe distances within chains is relatively large. However, the Fe-U interatomic distances are relatively small, and considerable d-f hybridization might be expected. As can be seen from Fig. 1, the U atoms are in planes with Fe atoms between the planes; the Fe atoms are widely separated and form chains perpendicular to the U planes. The U-U distances in the xy plane are small, but the distance between planes is large, giving rise to a cluster or planer structure. There is considerable delocalization of the uranium $5f$ electrons, i.e., bonding of U to U atoms within the xy planes. Engelhardt[17] finds that neither c/a nor the unit-cell volume follow T_c across the U_6X (X=Mn,Fe,Co,Ni) series. Moreover, the a and c directions are different with respect to their relationship to T_c in that a correlation is found between T_c and the basal-plane lattice parameter a, but not between c and T_c. T_c rapidly increases as a, the lattice parameter, decreases. Since T_c may be a strongly increasing function of U-U overlap, as discussed by Hill and Matthias,[2] then the a distance is of critical importance, as it determines both the closest U-U distance and it can also determine the U-Fe distance; d-f hybridization may be as important as f-f hybridization.[18] Hence, the low-temperature behavior of the lattice parameters is of vital importance to understanding the superconducting properties of the U_6X system.

The superconducting transition temperature was measured by means of a resonant detector bridge at 900 Hz and found to be 3.76±0.17 K. The sample for the Mössbauer measurement was made with 90% enriched ^{57}Fe and sealed in a cold-setting plastic. Transmission ^{57}Fe Mössbauer spectra were obtained using a 50-mCi ^{57}Co in Rh source held at 273.6 K.

MÖSSBAUER EFFECT

Mössbauer-effect measurements at ^{57}Fe in U_6Fe have been made between 4.3 and 300 K (see Fig. 2). The spectra are symmetric doublets to within 1% at all temperatures with no temperature dependence to the relative in-

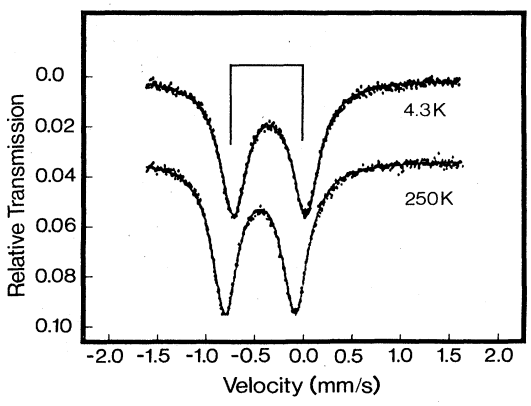

FIG. 2. Mössbauer spectra at 250 and 4.3 K.

tensities.[19] This behavior indicates vibrational isotropy between $\langle z^2 \rangle$ and $\langle x^2 \rangle$ in the tetragonal structure and any asymmetry is attributed to a very small quantity (less than one-half percent) of a second phase. Spectra characteristic of UFe_2 are not observed, confirming the x-ray result. The second phase may be due to a very small quantity of Fe in UO_2 at the surface of the particles of powdered U_6Fe, or in solution in γ- or β-U.

In an earlier study Blow[20] examined U_6Fe and Pu_6Fe at 26, 82, and 295 K by means of the ^{57}Fe Mössbauer effect. The results for U_6Fe yield a quadrupole splitting and shift approximately in agreement with the present study. However, a large asymmetry was observed in the doublet with the line at higher energy having greater intensity. The latter line width was also considerably greater than that at lower energy, a result not expected if the asymmetry was due to anisotropic lattice vibrations. We have observed similar results on unannealed samples crushed in air, and we attribute the asymmetry to a second phase; this impurity phase is not UFe_2 which can be detected via its magnetic transition at ≈ 160 K,[21] but is more probably a compound of uranium, iron, and oxygen. Boolchand[22] and Lemon *et al.*[23] have also made temperature-dependent Mössbauer measurements on this system; their values of quadrupolar splitting and shift are, within the reported experimental error, in agreement with those reported in this study. However, neither the phonon or electronic changes, nor the structural change observed in the present study by Mössbauer-effect and neutron-diffraction measurements are reported by Lemon *et al.*[23]

The centroid of the pattern, the Mössbauer shift, is a sum of two components; a thermal shift, which is proportional to the integral over the lattice specific heat, and an isomer shift, which reflects the number and character of the valence electrons. The thermal shift $\delta(T)$ is proportional to the mean-squared velocity of the Mössbauer atom, and through model calculations it can be related to positive moments of the phonon distribution $F(\omega)$.[24,25] For example, using a Debye formulation for the Fe vibrational motion, $\delta(T)-\delta(0)$ is a measure of the change in thermal energy characterized by a Debye temperature Θ_δ; Θ_δ is determined by $\langle \omega \rangle$ at low temperatures and $\langle \omega^2 \rangle$ at intermediate temperatures. Figure 3 shows the data for the temperature dependence of the shift. The solid curve is the result of fitting the data between 100 and 300 K to a Debye model with $\Theta_\delta = 451$ K. It is evident that the variation in shift with temperature is not characteristic of harmonic behavior; there is a deviation from Debye behavior below 100 K, which indicates either a softening in the iron vibrational modes, or a decrease in s character in the conduction-electron concentration, probably due to increased d occupation of iron.

The Mössbauer absorption A is proportional to the Debye-Waller factor in a harmonic solid

$$-\ln A \propto K^2 \langle r^2 \rangle \ , \tag{1}$$

where K is the wave vector of γ radiation.[26] At high temperature, the mean-squared displacement is linear in temperature and is proportional to Θ_f^{-2}, where Θ_f is the effective Debye temperature characterizing the Mössbauer spectral area measurements. Hence, the slope of $-\ln A$ versus T is very sensitive to the value of the Debye temperature. Figure 4 shows the temperature dependence of $-\ln A$ versus T for U_6Fe. The solid lines are least-squares fits to Debye models; above 100 K, $\Theta_f = 332$ K. As usual, Θ_f ($\propto \langle r^2 \rangle$) is different from Θ_δ ($\propto \langle v^2 \rangle$) due to the fact that these parameters are related to different moments of the Fe vibrational spectral density, with $\langle r^2 \rangle$ weighting the low-frequency phonons and $\langle v^2 \rangle$ the high-frequency phonons. The Mössbauer absorption, however, is dependent only on the behavior of the temperature dependence of the phonon spectrum and does not directly involve changes in the number and character of the electrons as does the shift. Hence, the jump in the magnitude of the Mössbauer absorption between 100 and 80 K with decreasing T is due to a hardening of the vibrational modes involving the Fe atoms from an effective Debye temperature of $\Theta_f = 332$ K to $\Theta_f = 400$ K. That is, a dramatic shift to high energy in the Fe phonon spectral density appears to occur below 100 K. Taking $\Theta_f \approx 400$ K for Fe at low temperature, and using a superposition of Debye temperatures weighted by the number of Fe and U

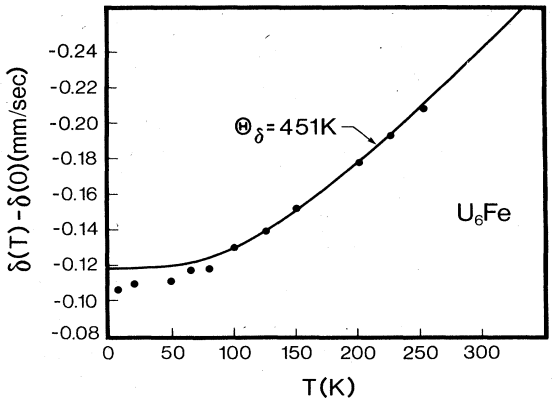

FIG. 3. Change in Mössbauer shift $\delta(T)-\delta(0)$ vs temperature for Fe in U_6Fe. The data fit a Debye model with $\Theta_\delta = 451$ K above 100 K. The deviation from harmonic behavior at ≈ 100 K is discussed in the text. [$\delta(0) = -0.23$ mm/sec; shift relative to $CaSnO_3$ at 273.6 K.]

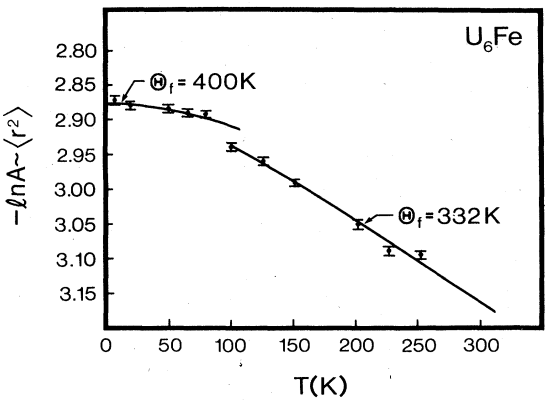

FIG. 4. Temperature dependence of the Mössbauer absorption A plotted as $-\ln A$ vs T. The solid lines are Debye model fits to $\Theta_f = 400$ K for $T < 100$ K and $\Theta_f = 332$ K for $T > 100$ K.

atoms in the compound, the Debye temperature for U is $\Theta \sim 80$ K; that is, the uranium vibrational modes are considerably softer than the heat-capacity Debye temperature ($\Theta = 125$ K) of the compound U_6Fe.[4]

The nonharmonic behavior of the Mössbauer shift at 100 K is opposite to the result from the mean-squared displacement and is probably due to a change in the valence character of the Fe. That is, there is an increase in the number (≈ 0.02) of d electrons (with a concomitant decrease in the number of s electrons) in the Fe valence band and a hardening of its vibrations below 100 K.

The Fe atom has noncubic site symmetry, which leads to a quadrupole splitting as shown in Fig. 5. The magnitude of the splitting E_Q is due to the electric field gradient tensor and arises in a metal largely from the character and density of electrons in the volume region of the nucleus.[26] One expects a small and smooth change with temperature due to thermal expansion and the effect of the Fermi function on the population of the electrons at the Fermi surface. As can be seen from Fig. 5, E_Q also changes abruptly. The observed change is similar in character to that of the other Mössbauer parameters.

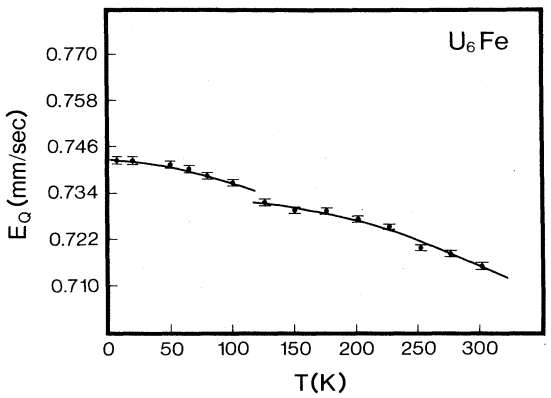

FIG. 5. Quadrupole splitting of ^{57}Fe in U_6Fe as a function of temperature.

NEUTRON DIFFRACTION

For the neutron-diffraction measurements, a 25-g sample of powdered U_6Fe was loaded with one atmosphere (at room temperature) of helium exchange gas into a 13.7-mm-diam, 57-mm-long vanadium can with an indium gasket seal. All of the sample handling, including grinding, was done in glove bags in inert atmosphere to prevent exposure to oxygen. The sample was cooled by a Displex (Air Products and Chemicals, Inc.) closed-cycle helium refrigerator. Data were collected at six temperatures between 20 and 295 K for about 10 h at each temperature using the Special Environment Powder Diffractometer (SEPD) at Argonne National Laboratory's Intense Pulsed Neutron Source.[27]

The data were analyzed by the Rietveld structural refinement technique[28] to obtain accurate structural parameters at each temperature. The results of these refinements are summarized in Table I. The ratio of the weighted profile R value R_{wp} to the expected R value based on counting statistics, R_{exp}, is a measure of the goodness of fit. The R values listed in Table I show that

TABLE I. Structural parameters for U_6Fe versus temperature. Tetragonal space group $I4/mcm$, with U(1) at $x\,x+\frac{1}{2}\,0$; U(2) at $xy0$; Fe at $00\frac{1}{4}$. The anisotropic temperature factor has the form $\exp(-b_{11}h^2-b_{22}k^2-b_{33}l^2-2b_{12}hk-2b_{13}hl-2b_{23}kl)$. The b_{ij}'s not included in the table are zero by symmetry.

Parameter	Temperature 20 K	50 K	100 K	150 K	220 K	295 K
a (Å)	10.2499(1)	10.2536(1)	10.2625(1)	10.2724(1)	10.2863(1)	10.3022(1)
c (Å)	5.2500(1)	5.2484(1)	5.2458(1)	5.2436(1)	5.2410(1)	5.2386(1)
V (Å^3)	551.56(1)	551.80(1)	552.49(1)	555.32(1)	554.54(1)	555.99(1)
x [U(1)]	0.4054(1)	0.4055(1)	0.4056(1)	0.4055(1)	0.4053(1)	0.4050(1)
$b_{11}=b_{22}$ [U(1)]	0.0008(1)	0.0009(1)	0.0010(1)	0.0012(1)	0.0017(1)	0.0021(1)
b_{33} [U(1)]	0.0007(3)	0.0008(3)	0.0006(3)	0.0008(3)	0.0011(4)	0.0021(4)
b_{12} [U(1)]	−0.0004(1)	−0.0005(1)	−0.0006(1)	−0.0006(1)	−0.0008(1)	−0.0010(1)
x [U(2)]	0.2148(1)	0.2148(1)	0.2145(1)	0.2143(1)	0.2140(1)	0.2136(1)
y [U(2)]	0.1027(1)	0.1026(1)	0.1029(1)	0.1031(1)	0.1032(1)	0.1036(1)
b_{11} [U(2)]	0.0008(1)	0.0008(1)	0.0009(1)	0.0011(1)	0.0014(1)	0.0017(1)
b_{22} [U(2)]	0.0006(1)	0.0007(1)	0.0008(1)	0.0010(1)	0.0013(1)	0.0016(1)
b_{33} [U(2)]	0.0034(3)	0.0035(3)	0.0046(3)	0.0054(3)	0.0070(4)	0.0090(4)
b_{12} [U(2)]	−0.000 16(5)	−0.000 16(6)	−0.000 22(6)	−0.000 18(7)	−0.000 27(7)	−0.000 15(8)
$b_{11}=b_{22}$ (Fe)	0.0007(1)	0.0009(1)	0.0010(1)	0.0012(1)	0.0017(1)	0.0019(1)
b_{33} (Fe)	0.0014(4)	0.0011(4)	0.0008(4)	0.0018(5)	0.0028(5)	0.0037(5)
R_{wp}[a] (%)	5.56	5.72	5.61	5.54	5.47	5.33
R_{expt}[a] (%)	2.49	2.87	2.89	2.88	3.11	2.80

[a]These quantities are defined in H. M. Rietveld, J. Appl. Crystallogr. 2, 65 (1969); J. D. Jorgensen and F. J. Rotella, *ibid.* 15, 27 (1982).

the structural refinements converged equally well at all temperatures using the previously determined tetragonal, $I4/mcm$, space group.[17,29]

As shown in Fig. 1(a), the structure of U_6Fe is body-centered tetragonal, with Fe atoms in high-symmetry positions at $00\frac{1}{4}$ and uranium atoms in two inequivalent positions at $x\,x+\frac{1}{2}\,0$ and $xy0$. Thus, all of the uranium atoms lie in planes at $z=0$ and $z=\frac{1}{2}$ with the Fe atoms halfway between the planes. At room temperature the U—U bond lengths range from 2.663 to 3.38 Å. This unusually large spread of bond lengths is similar to that observed in α-U where each uranium atom has two near neighbors at 2.76 Å, two at 2.85 Å, four at 3.276 Å, and four more at 3.36 Å.[30] Thus, the degree of bonding anisotropy observed in U_6Fe is not unexpected for f-electron systems. The short U—U bonds, 2.663 Å, 2.768 Å, and 2.841 Å, all lie in the xy plane forming rectangular, planar clusters of six uranium atoms (Fig. 1). The bonds which join uranium atoms in the layer at $z=0$ with those in the layer at $z=\frac{1}{2}$ are all significantly longer with the exception of a 3.07-Å U—U bond between U(2) atoms of different layers. This bond is quite close to the sum of metallic radii for uranium, 3.096 Å, based on Zachariasen's average radius for β-U.[31]

One reason for collecting neutron-diffraction data at low temperature was to investigate the possible occurrence of a structural phase transition around 100 K, where the anomaly in the Mössbauer spectra was observed. These neutron-diffraction results show no obvious evidence for a structural phase transition. In particular, no peak broadening, which would indicate a small departure from the room-temperature tetragonal symmetry, was observed at low temperature and no superlattice reflections could be seen in the powder data. Thus, if a structural phase transition occurs, it is too subtle to detect by powder methods.

The temperature-dependent structural data do reveal a pronounced thermal expansion anisotropy shown in Fig. 6; the c axis *expands* significantly with decreasing temperature while the sign of the a-axis thermal expansion is normal. The volume expansion is positive and is almost linear, except at the lowest temperatures, as shown in Fig. 6. Individual U—U bond lengths exhibit the same degree of thermal expansion anisotropy and allow a microscopic structural explanation for the behavior shown in Fig. 6. Selected bond lengths versus temperature are listed in Table II. The thermal expansion behavior is dominated by the contraction of the planar clusters of six uranium atoms shown in Fig. 1. The strong U—U bonds in this cluster shorten about 1% upon cooling to 20 K. This is roughly double the rate of the a-axis thermal contraction. The contraction of these planar clusters gives rise to a de-

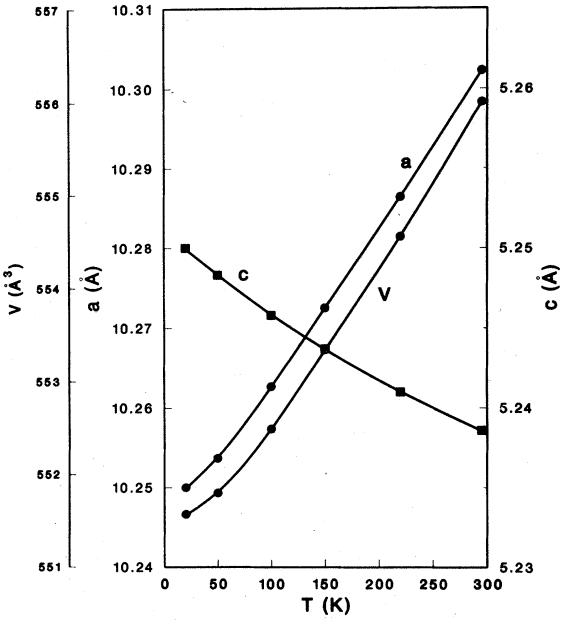

FIG. 6. Tetragonal unit-cell edges a and c and unit-cell volume for U_6Fe versus temperature.

TABLE II. Bond lengths (Å) in U_6Fe versus temperature. Numbers in parentheses are standard deviations of the last significant digit.

Bond	Temperature 20 K	50 K	100 K	150 K	220 K	295 K
U(1)—U(1)	2.741(2)	2.740(2)	2.740(2)	2.747(2)	2.754(3)	2.768(3)
	3.263(1)	3.262(1)	3.261(1)	3.263(1)	3.265(2)	3.270(2)
U(1)—U(2)	2.812(1)	2.812(2)	2.819(2)	2.824(2)	2.831(2)	2.841(2)
	3.274(1)	3.274(1)	3.276(1)	3.277(1)	3.278(1)	3.280(1)
	3.339(1)	3.342(2)	3.343(2)	3.341(2)	3.341(2)	3.337(2)
	3.893(1)	3.894(2)	3.900(2)	3.907(2)	3.916(2)	3.930(2)
U(2)—U(2)	2.646(2)	2.647(2)	2.651(2)	2.652(2)	2.658(2)	2.663(3)
	3.087(1)	3.088(1)	3.083(1)	3.080(1)	3.076(1)	3.071(1)
	3.365(1)	3.364(1)	3.367(1)	3.371(2)	3.373(2)	3.379(2)
	3.451(1)	3.452(1)	3.452(1)	3.455(2)	3.457(2)	3.459(2)
U(2)—Fe	2.771(1)	2.771(1)	2.771(1)	2.773(1)	2.773(1)	2.774(1)

crease in the angle θ [defined in Fig. 1(c)] from 25.87(3)° at 295 K to 25.55(3)° at 20 K. Thus, alternate U_4Fe_2 octahedra rotate in opposite directions around the c axis and at the same time elongate slightly (with the U—Fe bond length remaining nominally constant) producing the negative thermal expansion along c.

The phonon anomaly observed in the ^{57}Fe Mössbauer results is also seen in the Fe Debye-Waller factor from the diffraction data. The anisotropic components of the Debye-Waller factors for the U(1), U(2), and Fe atoms along the major and minor axes of the displacement ellipsoids are plotted in Fig. 7. When the anisotropic tensors are diagonalized, the Fe displacement thermal ellipsoid has two major axes parallel to the a and b crystallographic directions and a minor axis parallel to c. The major axis for U(1) is in the xy plane along the direction of the short U(1)—U(2) bond as shown in Fig. 1, while one minor axis is in the xy plane perpendicular to the major axis and the other is along c. The major axis for U(2) is parallel to c, and the minor axes are in the xy plane oriented as shown in Fig. 1.

The Debye-Waller factors from a diffraction experiment represent the combined static and thermal displacements of the atoms since the diffraction measurement probes the time and spatial average of the structure. Around 100 K, the c-axis component of the displacement tensor for Fe, U_3^2(Fe), goes through an unusual minimum. The Mössbauer results show a sudden reduction in the *thermal* vibrational amplitude at this temperature. Conversely, the diffraction results show an increasing *total* displacement along the c axis below 100 K for Fe. The most probable explanation is that below 100 K the Fe atom becomes localized in a site which is statically displaced from the average position $(0,0,\frac{1}{4})$. The magnitude of this displacement is about 0.03 Å based on the total mean-squared displacement from the refinement. If the direction of the displacement is random, the symmetry of the $I4/mcm$ space group is not violated. If the displacement is ordered, a charge-density-wave supercell or modulated structure is present, but the superlattice or satellite reflections are too weak to observe in the powder data.

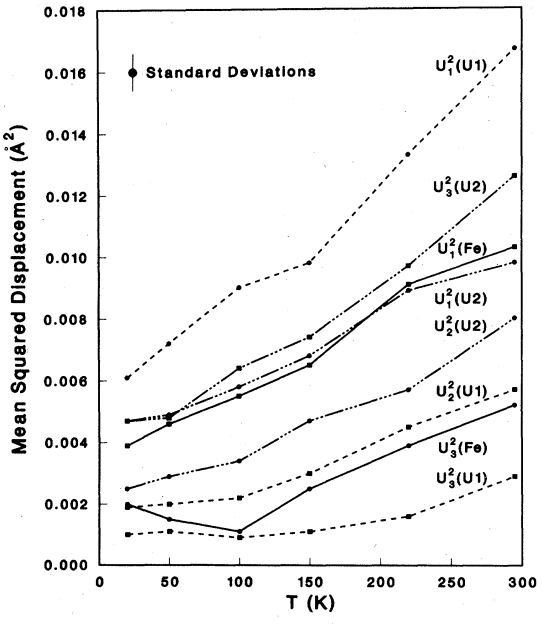

FIG. 7. Mean-squared displacements for U(1), U(2), and Fe atoms in U_6Fe versus temperature. In all cases, U_3 is along the crystallographic c axis. For Fe, $U_1^2 = U_2^2$ and U_1 and U_2 are parallel to the a and b axes, respectively. For atoms U(1) and U(2), the components U_1 and U_2 are in the xy plane with the orientations shown in Fig. 1 and described in the text.

Other features of the U_6Fe total displacement tensors versus temperature are also anomalous and suggest that the $I4/mcm$ tetragonal space group may not provide an accurate description of the structure on the local scale (even though it appears to be a valid model for the time- and spatially-averaged structure). The Mössbauer results for Fe show that the thermal vibrations for Fe are nearly isotropic at all temperatures. By comparison, the diffraction data show a pronounced anisotropy with U_1^2(Fe) > U_3^2(Fe) (note that for Fe, $U_1^2 = U_2^2$ by symmetry). However, the temperature dependence for U_1^2(Fe) and U_3^2(Fe) is nominally the same, in agreement with the Mössbauer results. This implies that static displacements of the Fe atoms U(Fe) $\cong 0.1$ Å in the xy plane are present at all temperatures. Such behavior would be similar to that observed for the metal ion M in the Chevrel-phase compounds, MMo_6S_8, which have also been investigated by using both Mössbauer measurements and neutron-diffraction measurements.[32,33]

Several of the components of the U(1) and U(2) atom-displacement tensors also remain unusually large at low temperature, suggesting that static displacements or pronounced anharmonic vibrational motions are also present for the uranium atoms (at all temperatures). Again, if these static displacements are ordered, the actual structure may be a supercell of $I4/mcm$. If this is the case, the superlattice reflections are too weak to observe by powder-diffraction techniques. A single-crystal study is required to resolve this question.

With regard to the possible existence of subtle variations from the average body-centered-tetragonal structure of U_6Fe, it is instructive to consider the low-temperature charge-density-wave transition in alpha-uranium. In this case, the existence of a structural anomaly at 43 K was very clear from elastic constant, heat capacity, magnetic susceptibility, thermal expansion and diffraction results.[34] A number of neutron-diffraction experiments were performed on different crystals to search for extra reflections along principal zone axes.[35] None were found, and the main conclusions of the first full crystallographic investigation of alpha-uranium were that changes in Bragg intensities at 43 K were due to a reversible change in crystal perfection, and that the thermal vibration along the [001] direction was much greater at low temperature than along the other axes. The charge density wave satellite reflections were not found until the neutron Laue technique was employed to provide a continuous probe of reciprocal space.[36] The same technique should be used to throughly investigate the U_6Fe structure.

SUMMARY

From the temperature dependence of the Mössbauer absorption, phonon shifting is found to occur between 80 and 100 K; the Fe lattice hardens at low temperature from $\Theta_f = 332$ K above 100 K to $\Theta_f = 400$ K below 100 K. The Debye temperature for U in the compound U_6Fe is then calculated to be 80 K; that is, U is softer than the average Debye temperature measured in heat capacity for the compound. The Mössbauer shift also undergoes an anomalous change in the same temperature region. The change in shift below 100 K is opposite in sign to that expected from phonon hardening and is attributed to a change in the electronic structure of the Fe atom; namely, an increase in *d* occupation (decrease in *s* occupation). Neutron-diffraction measurements indicate that the temperature dependence of the total Debye-Waller factor is anisotropic and that the basal plane lattice parameter strongly contracts at low temperature, decreasing the U-U distances and increasing U hybridization. The *c* axis is found to have a negative coefficient of thermal expansion which, with decreasing temperature, leads to increased separation of both the *xy* planes and the U clusters in the *xy* planes. The interatomic distance between Fe and U is small and hence a large *d-f* hybridization is expected which may also be playing an important role in determining the superconducting properties of U_6Fe.

Combining the neutron-diffraction results with the Mössbauer measurements, a static displacement of Fe atoms is inferred which is along the *c* axis and grows with decreasing temperature. Moreover, the temperature dependence of the anisotropic components of the Debye-Waller factors derived from the diffraction results suggests other static displacements for both U and Fe atoms at all temperatures. A careful single-crystal diffraction experiment is needed to check for possible supercells or modulated structures which cannot be seen in the powder data.

ACKNOWLEDGMENTS

It is a pleasure to thank Lance DeLong, Punit Boolchand, and B. D. Dunlap for enlightening discussions. This work was partially supported by the National Science Foundation, Grant No. DMR-84-16695, and by the U.S. Department of Energy.

[1]B. S. Chandrasekhar and J. K. Hulm, J. Phys. Chem. Solids **7**, 259 (1958).

[2]H. H. Hill and B. T. Matthias, Phys. Rev. **168**, 464 (1968).

[3]F. Steglich, J. Aarts, C. D. Bredl, W. Lieke, D. Mescheda, W. Franz, and H. Schäfar, Phys. Rev. Lett. **43**, 1892 (1979).

[4]L. E. DeLong, J. G. Huber, K. N. Yang, and M. B. Maple, Phys. Rev. Lett. **51**, 312 (1983).

[5]H. R. Ott, H. Rudigier, Z. Fisk, and J. L. Smith, Phys. Rev. Lett. **50**, 1595 (1983).

[6]F. Steglich, J. Aarts, C. D. Bredl, G. Cordier, F. R. de Boer, W. Lieke, and V. Raunschwalle, in *Superconductivity in d- and f-Band Metals,* edited by W. Buckel and W. Weber (Kernforschungszentrum Karlsruhe *GmbH,* Karlsruhe, 1982), p. 145.

[7]E. Bucher, J. P. Maita, G. W. Hull, R. C. Fulton, and A. S. Cooper, Phys. Rev. B **11**, 440 (1975).

[8]C. M. Varma, Bull. Am. Phys. Soc. **29**, 404 (1984).

[9]G. R. Stewart, Z. Fisk, J. O. Willis, and J. L. Smith, Phys. Rev. Lett. **52**, 679 (1984).

[10]J. W. Chen, S. E. Lambert, M. B. Maple, Z. Fisk, J. L. Smith, G. R. Stewart, and J. O. Willis, Phys. Rev. B **30**, 1583 (1984).

[11]R. W. White, J. D. G. Lindsay, and R. D. Fowler, Solid State Commun. **13**, 531 (1973).

[12]J. J. Englehardt, Solid State Commun. **13**, 1355 (1973).

[13]R. O. Eliot, J. L. Smith, R. S. Finoccharo, and D. A. Koss, Mater. Sci. Eng. **49**, 65 (1981).

[14]M. B. Brodsky, Phys. Rev. B **9**, 1381 (1974).

[15]D. J. Lam, J. B. Darby, Jr., and M. V. Nevitt, in *The Actinides: Electronic Structure and Related Properties,* edited by A. J. Freeman and J. B. Darby, Jr. (Academic, New York, 1974), Vol. 2, Chap. 4.

[16]R. F. Domagada, C. Steves, F. J. Kavasek, and A. E. Dwight, J. Nucl. Mater. **119**, 351 (1983).

[17]J. J. Engelhardt, J. Phys. Chem. Solids **36**, 123 (1975).

[18]D. Koelling (private communication).

[19]P. P. Vaishnava, C. A. Strelecky, A. E. Dwight, C. W. Kimball, and F. Y. Fradin, in *17th International Conference on Low Temperature Physics,* edited by U. Eckern, A. Schmid, W. Weber, and H. Wühl (North-Holland, Amsterdam, 1984), p. 331.

[20]S. Blow, J. Phys. Chem. Solids **30**, 1549 (1969).

[21]A. T. Aldred, J. Magn. Magn. Mater. **10**, 421 (1979).

[22]P. Boolchand (private communication).

[23]G. Lemon, P. Boolchand, M. Stevens, M. Marcuso, L. E. DeLong, and J. G. Huber, Bull. Am. Phys. Soc. **29**, 405 (1984).

[24]T. A. Kitchens, P. P. Craig, and R. D. Taylor, in *Mössbauer Effect Methodology,* edited by I. Gruverman (Plenum, New York, 1969), Vol. 5, p. 123.

[25]C. W. Kimball, L. W. Weber, and F. Y. Fradin, Phys. Rev. B **14**, 2769 (1976).

[26]V. I. Goldanskii and E. F. Makarov, in *Chemical Applications of Mössbauer Spectroscopy,* edited by V. I. Goldanskii and R. H. Herber (Academic, New York, 1968), p. 1.

[27]J. D. Jorgensen and J. Faber, Jr., in Proceedings of the Sixth Meeting of the International Collaboration on Advanced Neutron Sources, Argonne National Laboratory Report No. ANL-82-80, 1983 (unpublished), p. 105.

[28]R. B. VonDreele, J. D. Jorgensen, and C. G. Windsor, J. Appl. Crystallogr. **15**, 581 (1982).

[29]N. C. Baezinger, R. E. Rundle, A. I. Snow, and A. S. Wilson, Acta Crystallogr. **3**, 34 (1950).

[30]C. W. Jacob and B. E. Warren, J. Am. Chem. Soc. **59**, 2588 (1937).

[31]W. H. Zachariasen, J. Inorg. Nucl. Chem. **35**, 3487 (1973).

[32]J. D. Jorgensen, D. G. Hinks, D. R. Noakes, P. J. Viccaro, and G. K. Shenoy, Phys. Rev. B **27**, 1465 (1983).

[33]K. Yvon, *Current Topics in Material Science,* edited by E. Kaldis (North-Holland, Amsterdam, 1979), Vol. 3, pp. 53—129; Solid State Commun. **25**, 327 (1978).

[34]G. H. Lander, J. Magn. Magn. Mater. **29**, 271 (1982), and the references cited therein.

[35]G. H. Lander and M. H. Mueller, Acta Crystallogr. Sect. B **26**, 129 (1970).

[36]J. C. Marmeggi and A. Delapalme, Physica **102B**, 309 (1980).